ARTICLE



Solution NMR backbone assignments of the N-terminal Z α -linker-Z β segment from *Homo sapiens* ADAR1p150

Parker J. Nichols¹ · Morkos A. Henen¹,² · Quentin Vicens¹ · Beat Vögeli¹ ©

Received: 28 January 2021 / Accepted: 10 March 2021 © The Author(s), under exclusive licence to Springer Nature B.V. 2021

Abstract

Adenosine-to-inosine (A-to-I) editing of a subset of RNAs in a eukaryotic cell is required in order to avoid triggering the innate immune system. Editing is carried out by ADAR1, which exists as short (p110) and long (p150) isoforms. ADAR1p150 is mostly cytoplasmic, possesses a Z-RNA binding domain ($Z\alpha$), and is only expressed during the innate immune response. A structurally homologous domain to $Z\alpha$, the $Z\beta$ domain, is separated by a long linker from $Z\alpha$ on the N-terminus of ADAR1 but its function remains unknown. $Z\beta$ does not bind to RNA in isolation, yet the binding kinetics of the segment encompassing $Z\alpha$, $Z\beta$ and the 95-residue linker between the two domains ($Z\alpha$ – $Z\beta$) are markedly different compared to $Z\alpha$ alone. Here we present the solution NMR backbone assignment of $Z\alpha$ – $Z\beta$ from H. Sapiens ADAR1. The predicted secondary structure of $Z\alpha$ – $Z\beta$ based on chemical shifts is in agreement with previously determined structures of $Z\alpha$ and $Z\beta$ in isolation, and indicates that the linker is intrinsically disordered. Comparison of the chemical shifts between the individual $Z\alpha$ and $Z\beta$ domains to the full $Z\alpha$ – $Z\beta$ construct suggests that $Z\beta$ may interact with the linker, the function of which is currently unknown.

Keywords ADAR1 \cdot Editing \cdot Z-RNA \cdot Protein structure and dynamics \cdot Protein domains \cdot Backbone chemical shift assignment

Biological context

Distinguishing between self and non-self RNA is critical in controlling the innate immune response. In humans, self RNAs are edited by an adenosine deaminase that acts on RNA (ADAR1), which converts adenosines to inosines (Bass and Weintraub 1988; Wagner et al. 1989; Nishikura 2016). ADAR1 is constitutively expressed in most cells as a stable p110 isoform localized in the nucleus (O'Connell and Keller 1994; O'Connell et al. 1995; Patterson and Samual 1995). Upon invasion by a pathogen, the cell launches an interferon (IFN) response, resulting in the expression of a longer p150 isoform, which contributes to resisting the

and Keller 1994; O'Connell et al. 1995; Patterson and Samual 1995; George and Samuel 1999) (Fig. 1a). A-to-I editing is therefore augmented during the IFN response, primarily through the action of ADAR1p150 (Chung et al. 2018). In addition to becoming cytoplasmic, ADAR1p150 is also distinct from ADAR1p110 due to the presence of a N-terminal Zα domain, which is a member of a family of helix-turnhelix domains that recognize the unusual geometry of the Z-conformation in DNA or RNA, and binds to five base pairs in a symmetrical fashion (Herbert et al. 1998; Schwartz et al. 1999b; Brown et al. 2000; Placido et al. 2007) (Fig. 1b).

infection by editing self RNAs in the cytoplasm (O'Connell

The $Z\beta$ domain of ADAR1, which is located C-terminal to $Z\alpha$ and separated by a flexible 95-residue linker, is structurally homologous to $Z\alpha$ (Athanasiadis et al. 2018) but lacks the critical Z-recognizing residues required for adoption of Z-DNA/RNA and B-Z/A-Z junctions (Athanasiadis 2012). In the following, we refer to the $Z\alpha$ -linker- $Z\beta$ segment as $Z\alpha$ - $Z\beta$. While $Z\beta$ does not bind to DNA/RNA in isolation, $Z\alpha$ - $Z\beta$ is characterized by markedly different Z-DNA/RNA binding kinetics (Schwartz et al. 1999a). $Z\beta$ is resistant to proteolysis only in the context of $Z\alpha$ - $Z\beta$ and the flexible linker between the two folded domains becomes

- Quentin Vicens quentin.vicens@cuanschutz.edu
- ☑ Beat Vögeli beat.vogeli@cuanschutz.edu

Published online: 19 March 2021

- Department of Biochemistry & Molecular Genetics, School of Medicine, University of Colorado, 12801 E. 17th Avenue, Aurora, CO 80045, USA
- Department of Pharmaceutical Organic Chemistry, Faculty of Pharmacy, Mansoura University, Mansoura 35516, Egypt



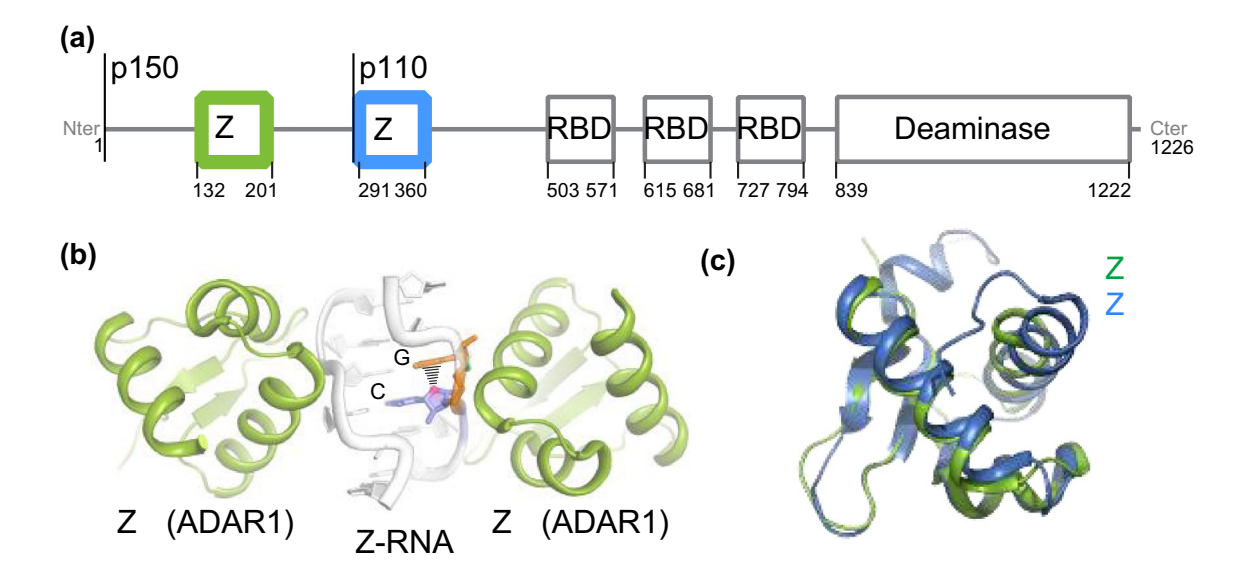


Fig. 1 The $Z\alpha$ and $Z\beta$ domains of ADAR1p150. **a** Domain organization of ADAR1: $Z\alpha$ and $Z\beta$ are structurally homologous helix-turnhelix DNA/RNA-binding domains, RBD stands for double-stranded RNA binding domain. Both isoforms are indicated. **b** Crystal structure of (CpG)₃ RNA bound to $Z\alpha$ from ADAR1 (PDB ID: 2GXB,

(Placido et al. 2007)). c Structural alignment of the Z α (PDB ID: 2GXB) and Z β (PDB ID: 1XMK, (Athanasiadis et al. 2018)) domains of ADAR1. The backbone RMSD between the two structures is 0.9 Å (excluding the termini)

resistant to proteolysis when bound to Z-DNA (Schwartz et al. 1999a). These findings led to the proposal that $Z\alpha$ – $Z\beta$ may undergo a large structural rearrangement when bound to Z-DNA/Z-RNA or that $Z\alpha$ – $Z\beta$ functions as a bipartite binding domain with $Z\beta$ gaining the ability to bind nucleic acid only in the context of $Z\alpha$ – $Z\beta$ (Schwartz et al. 1999a). Based on its crystal structure as a dimer with a cadmium ion at the interface, it was also proposed that $Z\beta$ may act as a dimerization domain (Athanasiadis et al. 2018). The exact role of $Z\beta$ thus remains elusive, although it is clear that $Z\alpha$, $Z\beta$, and the linker region in between the two domains act in concert.

Here we report the NH/ $C_{\alpha}/C_{\beta}/CO$ solution NMR backbone assignments of $Z\alpha$ – $Z\beta$ as well as the NH/ C_{α}/C_{β} chemical shifts for the individual $Z\alpha$ and $Z\beta$ domains from ADAR1. While the assignments of the $Z\alpha$ – $Z\beta$ and $Z\beta$ domains from ADAR1 are novel, the $Z\alpha$ domain has been characterized by NMR previously (Schade et al. 1999a, b), however, the chemical shifts for ADAR1 $Z\alpha$ have not been deposited to the BMRB until now.

Methods and experiments

Protein expression and purification

The N-terminal $Z\alpha$ domain of *Homo sapiens* ADAR1 in the pet-28a(+) plasmid (N-terminal $6 \times His$ -tag and thrombin cleavage site between His tag and the $Z\alpha$ sequence) was a gift from Drs. Peter Dröge and Alekos Athanasiadis. $Z\alpha$ – $Z\beta$

and Zβ were ordered from GenScript (cloned into the same expression vector, pet-28a(+)) and prepared in the same way as $Z\alpha$, which was expressed and purified similarly to (Placido et al. 2007; Kruse et al. 2020). Briefly, the plasmids were transformed and expressed in BL21(DE3) E. coli. The cell cultures were grown in M9 minimal media with 1 g/L ¹⁵N ammonium chloride and 1.5 g/L ¹³C glucose (Millipore-Sigma, Burlington, MA) to an optical density at 600 nm of 0.6, induced with IPTG at a final concentration of 1 mM, and allowed to express $Z\alpha$, $Z\beta$, or $Z\alpha$ – $Z\beta$ for 4 h at 37 °C, then centrifuged to collect the cell pellets. Pellets were resuspended in lysis buffer (50 mM Tris-HCl (pH 8.0), 300 mM NaCl, 10 mM Imidazole, 5 mM β-Mercaptoethanol (BME)) and sonicated. Lysate was centrifuged and the supernatant was applied to a His-trap column, washed with 40 mL of lysis buffer, 80 mL of wash buffer (50 mM Tris-HCl (pH 8.0), 1 M NaCl, 10 mM Imidazole, 5 mM BME), and eluted in 20 mL of elution buffer (50 mM Tris-HCl (pH 8.0), 300 mM NaCl, 500 mM Imidazole, 1 mM BME). The eluents were concentrated to ~2 mL and applied to a Hiload 16/600 Superdex 75 Gel Filtration Column (GE Healthcare) and the peak corresponding to pure protein was collected and concentrated using an Amicon 3 kDa cutoff centrifugal filter (Millipore-Sigma, Burlington, MA). At this step, $Z\alpha$ – $Z\beta$ and to a lesser extent also $Z\beta$ showed concentrationand salt-dependent oligomerization. To prevent aggregation, more NaCl was added (to a final concentration of 100 mM for NMR measurements), with the concentration of NaCl being dependent upon the concentration of protein. The



proteins were dialyzed and concentrated into the following buffers for NMR: 20 mM potassium phosphate (pH 6.4), 25 mM or 100 mM NaCl for Z α (2 mM protein), 20 mM potassium phosphate (pH 6.4), 25 mM NaCl or 100 mM NaCl for Z β (2 mM protein), 20 mM potassium phosphate (pH 6.4), 100 mM NaCl for Z α –Z β (680 μ M protein). D₂O was added to 5%. See Table 1 for specifics on which buffer was used for which NMR experiments.

Perdeuterated $Z\alpha$ – $Z\beta$ was prepared in the same way as non-perdeuterated $Z\alpha$ – $Z\beta$ except that the M9 minimal media culture contained 99.8% D_2O instead of water and had uniformly deuterated ^{13}C glucose (Cambridge Isotope Laboratories, Tewksbury, MA). Additionally, the *E. coli* were D_2O adapted before expression following the protocol from (Cai et al. 2016).

NMR spectroscopy

The TROSY backbone experiments for the assignment of $Z\alpha$ – $Z\beta$ and the HNCACB for the isolated $Z\alpha$ domain were carried out on a Bruker 600 MHz spectrometer equipped with a 5/3 mm triple resonance $^1H/^{13}C/^{15}N/^{19}F$ cryoprobe (CP2.1 TCI). All other experiments were done on a Varian 900 MHz spectrometer equipped with a 5 mm triple resonance $^1H/^{13}C/^{15}N$ cold probe with a Z-axis gradient.

¹⁵N-HSQC spectra of the individual Zα and Zβ domains were recorded both at 25 °C and with 25 mM NaCl, and at 35 °C with 100 mM NaCl. The ¹⁵N-HSQC of Zα–Zβ was recorded at 35 °C with 100 mM NaCl. All ¹⁵N-HSQC spectra were collected with 1024 (1 H)×120 (15 N) complex points, a 1.6 s recycle delay, and 16 scans. The spectral widths were 16 and 35 ppm for the 1 H and 15 N dimensions, respectively.

Assignment of the individual $Z\alpha$ and $Z\beta$ domains was achieved through HNCACB experiments measured at 25 °C and 25 mM NaCl with 1024 (1H)×96 (^{13}C)×80 (^{15}N) complex points (2306 of the points were collected following a 30% non-uniform sampling scheme from the Wagner website: http://gwagner.med.harvard.edu/intranet/hmsIST/gensc hed_new.html, (Hyberts et al. 2012)), a 1 s recycle delay, and 8 scans. The spectral widths were 15.6, 70, and 35 ppm for the 1H , ^{13}C , and ^{15}N dimensions, respectively.

Assignment of Zα–Zβ was achieved by measurement of 3D TROSY-HNCACB, 3D TROSY-HN(CO)CACB, 3D TROSY-HN(CA)CO, 3D TROSY-HNCO, and 3D HNN experiments on a perdeuterated sample. The four TROSY experiments were measured with $1024 (^{1}\text{H}) \times 96 (^{13}\text{C}) \times 80$ (15N) complex points (1274 of the points were collected following a 16% sampling scheme from the Wagner site), a 1.9 s recycle delay (except for the TROSY-HNCO, which had a delay of 1 s), and 16 scans. The spectral widths were 18 (¹H), 80 (¹³C), and 35 (¹⁵N) ppm for the TROSY-HNCACB and TROSY-HN(CO)CACB experiments, and 18 (1 H), 14 (13 C), and 35 (15 N) ppm for the TROSY-HN(CA) CO and TROSY-HNCO experiments. The HNN experiment was measured with $1024 \, (^{1}\text{H}) \times 96 \, (^{15}\text{N}) \times 80 \, (^{15}\text{N})$ complex points (1927 of the points were collected following a 25% NUS sampling scheme from the Wagner site), a 1 s recycle delay, and 16 scans. The spectral widths were 15.6 and 70 & 35 ppm for the ¹H, ¹³C, and ¹⁵N dimensions. The HNN experiment, which correlates ¹⁵N and ¹H^N of residue i with the ¹⁵N of residues of i+1 and i-1, was helpful for assigning overlapped regions of which there were many in the linker region of Zα–Zβ. Residues 205–212 have chemical shifts identical to those of residues 253-260, as they are part of a repeat sequence within the linker region (with the sequence NQHSGVVRP).

Table 1 NMR experiments and sample information

Construct identity	Measured NMR experiments	Field strength	Sample concentration	Sample temperature (°C)	Buffer conditions	Molecular weight (kDa)
Ζα	¹⁵ N-HSQC HNCACB	900 MHz 600 MHz	2 mM	25	20 mM potassium phosphate (pH 6.4), 25 mM NaCl	9.2
Ζα	¹⁵ N-HSQC	900 MHz	2 mM	35	20 mM potassium phosphate (pH 6.4), 100 mM NaCl	9.2
Ζβ	¹⁵ N-HSQC HNCACB	900 MHz 900 MHz	2 mM	25	20 mM potassium phosphate (pH 6.4), 25 mM NaCl	10.9
Ζβ	¹⁵ N-HSQC	900 MHz	2 mM	35	20 mM potassium phosphate (pH 6.4), 100 mM NaCl	10.9
Ζα–Ζβ	15N-HSQC TROSY-HNCACB TROSY-HN(CO)CACB TROSY-HN(CA)CO TROSY-HNCO HNN	900 MHz 600 MHz 600 MHz 600 MHz 600 MHz 900 MHz	680 μΜ	35	20 mM potassium phosphate (pH 6.4), 100 mM NaCl	27.2



The 3D NUS-spectra were constructed using the hmsIST software (Hyberts et al. 2012), and the linearly acquired 2D spectra were subject to NUS zero-filling as an alternative to linear prediction. A solvent subtraction function was applied in the direct dimension. Further data processing and visualization were performed using NMR-Pipe/NMRDraw (Delaglio et al. 1995) and NMRFAM Sparky (Lee et al. 2015). Resonance assignment was performed using the CCPNmr analysis software version 2.4.2 (Vranken et al. 2005).

Assignment and data deposition

Initial 3D experiments on ¹⁵N, ¹³C isotopically enriched Zα–Zβ at 25 °C only resolved peaks from the linker region and the flexible termini. Thus, we turned to ²H, ¹⁵N, ¹³C isotope labeling and measured TROSY versions of the standard suite of backbone experiments (Cavanagh 2007) at 35 °C, which had enough signal to be able to assign 98% of the entire $Z\alpha$ – $Z\beta$ construct (Table 2). The assignments of the $Z\alpha$ and $Z\beta$ domains in isolation were helpful in narrowing down the search area of the peaks within the full construct. While the backbone assignments of the $Z\alpha$ and Zβ domains were done at 25 °C, we were able to assign the ¹⁵N-¹H HSQC spectra measured at 35 °C through nearest neighbor assignment. The ¹⁵N-¹H HSQC of the three constructs and the peak assignments are shown (Fig. 2). We have deposited the chemical shifts for $Z\alpha$, $Z\beta$ and $Z\alpha$ – $Z\beta$ under BMRB accession numbers: 50,714, 50,713, and 50,715 respectively.

Chemical shift analysis

Several conclusions could immediately be drawn from the spectra and assignments of $Z\alpha$ – $Z\beta$. First, the linker between the $Z\alpha$ and $Z\beta$ domains is intrinsically disordered, as determined by its low chemical shift dispersion and favorable relaxation properties (Fig. 2). The Secondary Structure Propensity Score (SSP) (Marsh et al. 2006) of the linker region mostly fluctuates between 0 and 0.2 (a score of 1 indicates a fully formed α -helix, while -1

indicates a β -sheet), confirming that the linker is indeed intrinsically disordered with some potential α -helical propensity (Fig. 3). In addition, the SSP score shows that the secondary structure of the $Z\alpha$ and $Z\beta$ domains is well-folded and in agreement with the structures of the isolated domains ($Z\alpha$ PDB IDs: 2GXB (Placido et al. 2007), 1QGP (Schade et al. 1999a); $Z\beta$ PDB ID: 1XMK (Athanasiadis et al. 2018)) (Fig. 3). This suggests that the $Z\alpha$ and $Z\beta$ domains within the context of the larger $Z\alpha$ - $Z\beta$ construct adopt a similar structure as they do in isolation.

An overlay of the $Z\alpha$, $Z\beta$, and $Z\alpha$ – $Z\beta$ ¹⁵N-¹H HSQC shows that for the most part, the peaks from the $Z\alpha$ and $Z\beta$ domains in isolation match well to those within the context of $Z\alpha$ – $Z\beta$ (Fig. 4a). However, there are deviations between the constructs, especially in the $Z\beta$ domain. In order to investigate this in greater depth, we calculated Chemical Shift Perturbations (CSPs) (Montaville et al. 2008; Williamson 2013) between the isolated domains and the full construct (Fig. 4b) according to the following equation:

$$CSP = \sqrt{\left(\delta_{H,free} - \delta_{H,bound}\right)^2 + 0.2\left(\delta_{N,free} - \delta_{N,bound}\right)^2}$$

For the $Z\alpha$ domain, five residues showed CSPs above the noise level (we took the noise level to be at ~ 0.19) which included Lys154, Thr157, Thr167, Leu185, and Ser200 (Fig. 4b). The Zβ domain showed significantly more CSPs above the noise, with 15 residues including Glu297, Lys301, Asp304, Phe307, Ser310, Ile321, Leu323, Thr324, Ala326, Arg 327, Ile329, Asp330, Ile334, Arg338, and Thr347 (Fig. 4b). Plotting these residues on the structures of $Z\alpha$ and $Z\beta$ revealed that while their location on $Z\alpha$ appears to be random (and therefore difficult to determine whether they are of functional importance), on $Z\beta$, they collectively form a belt that stretches almost 360° around the protein (Fig. 4c). Such an interface suggests that $Z\beta$ may interact with the linker region of $Z\alpha$ – $Z\beta$ in some way, a hypothesis which we are planning to test in the near future.

Table 2 Backbone assignment statistics of $Z\alpha$, $Z\beta$, and $Z\alpha$ – $Z\beta$

Construct identity with numbering of relevant residues	Total number of relevant residues ^a	Total number of relevant non- proline residues	% backbone resonances assigned (number of backbone atoms assigned) ^b
Ζα (139–202)	64	61	97.6% (61 ¹⁵ N, 63 Cα, 57 Cβ)
Ζβ (290–365)	76	75	98.7% (74 ¹⁵ N, 75 Cα, 72 Cβ)
$Z\alpha - Z\beta (139 - 365)$	227	212	98.2% (208 15 N, 221 C α , 205 C β , 220 CO)

^aAll constructs have 20 extra non-relevant residues from cloning and the His-tag

^bBackbone assignment % as extracted from CCPNmr (Vranken et al. 2005)



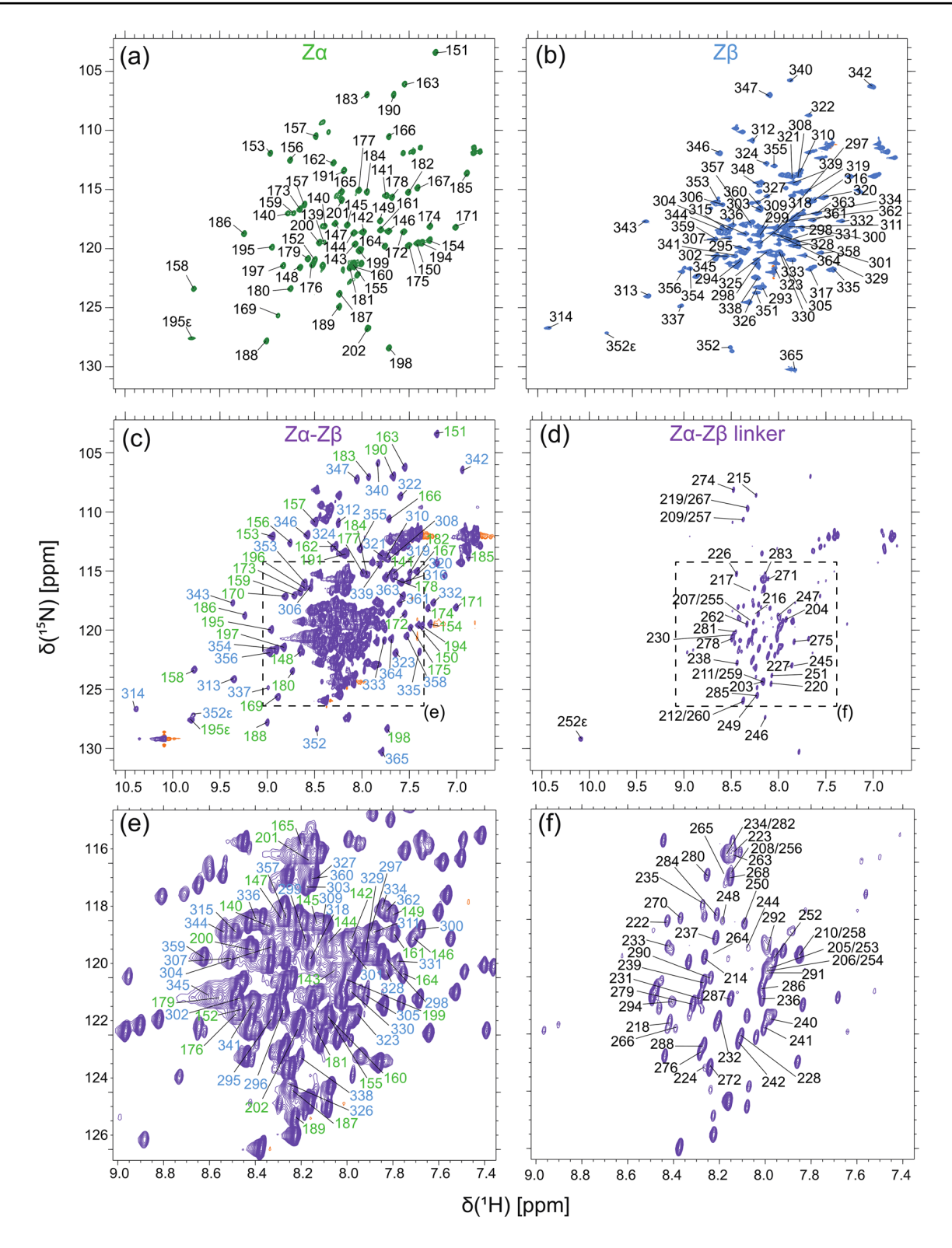
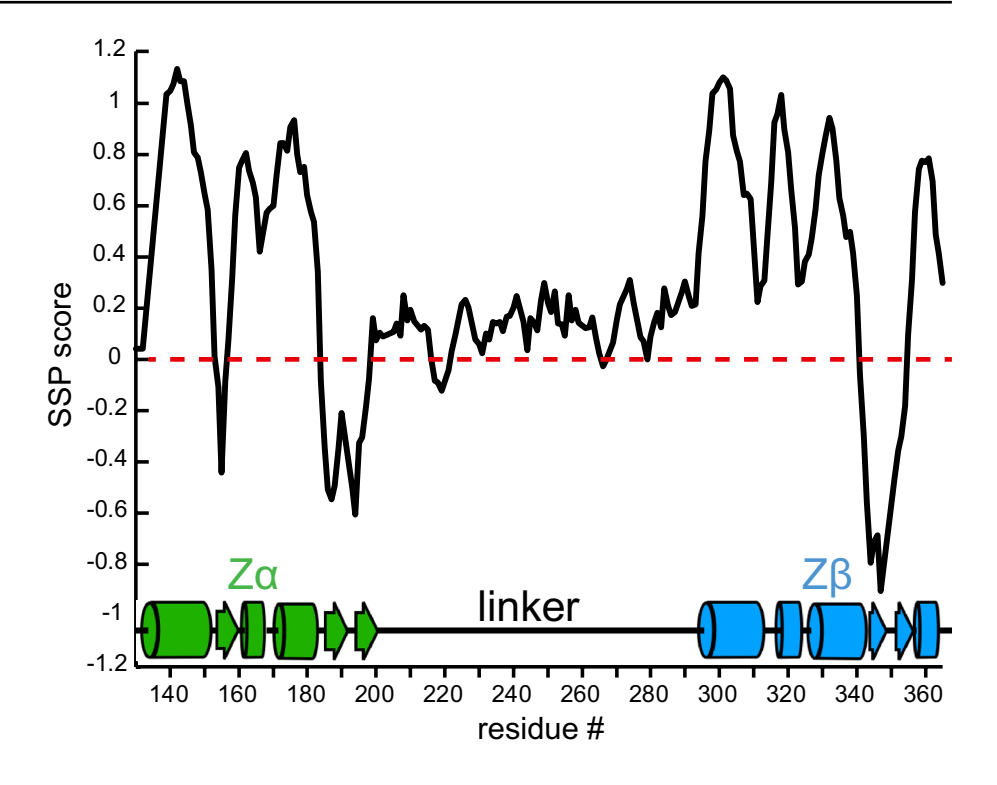


Fig. 2 Assigned $^{1}\text{H}^{-15}\text{N}$ HSQC spectra of $Z\alpha$, $Z\beta$, and $Z\alpha$ – $Z\beta$. Shown are the $^{1}\text{H}^{-15}\text{N}$ HSQC spectra of $Z\alpha$ (green, **a**), $Z\beta$ (blue, **b**), and $Z\alpha$ – $Z\beta$ (purple, **c** and **d**) measured at 900 MHz, 35 °C, and in 20 mM potassium phosphate (pH 6.4), 100 mM NaCl. The spectrum of $Z\alpha$ – $Z\beta$ in **c** has a low contour level cutoff, where only the $Z\alpha$ and

 $Z\beta$ domain assignments are shown in green and blue, respectively, and a high contour level cutoff in d to highlight the linker residues. e and f Blown-up regions from (c) and (d), respectively, to more clearly show the assignments within the crowded region of the spectra



Fig. 3 Secondary Structure Propensity Score of $Z\alpha$ – $Z\beta$ of ADAR1. The Secondary Structure Propensity score (SSP) calculated from the assigned HN, N, $C\alpha$, $C\beta$, and CO chemical shifts (Marsh et al. 2006) for $Z\alpha$ – $Z\beta$ is shown. The residue # is on the x-axis while SSP score is on the y-axis



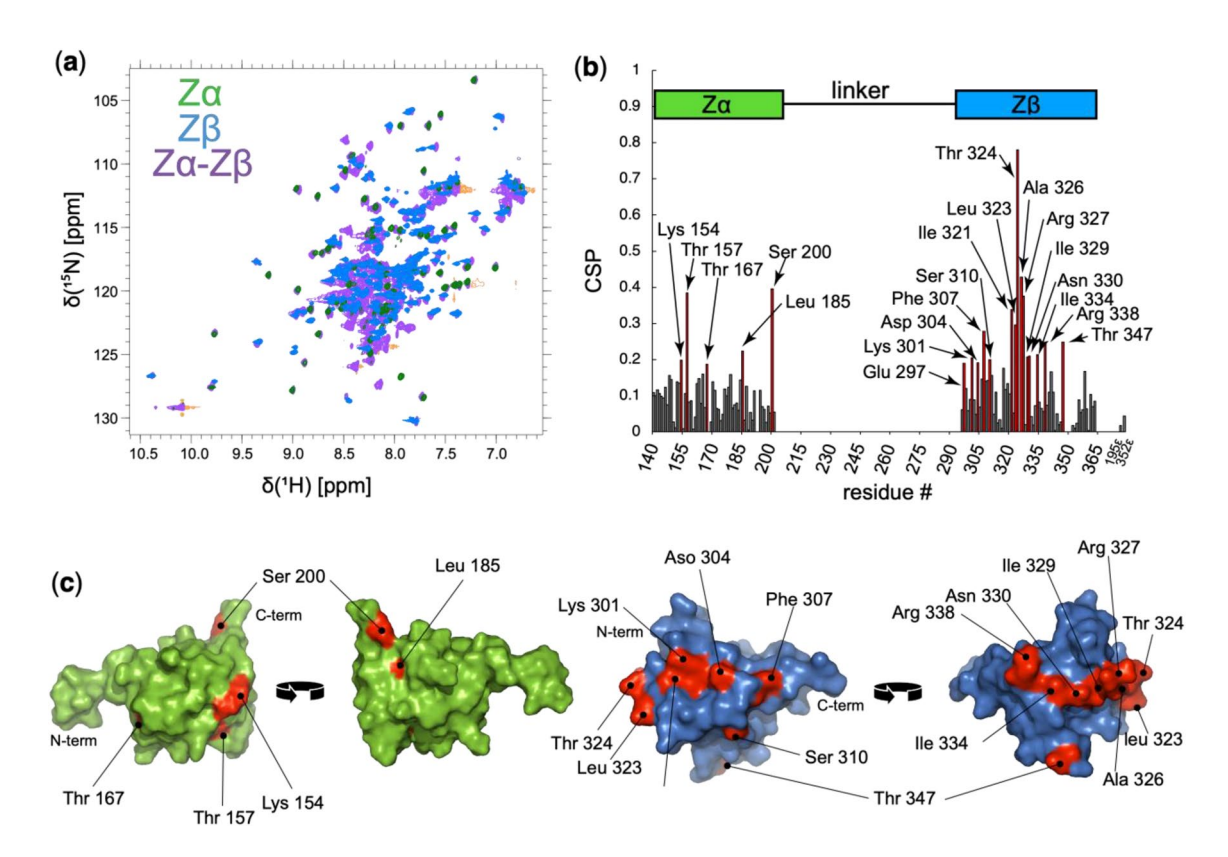


Fig. 4 Chemical shift perturbations between $Z\alpha$ and $Z\beta$ in isolation versus $Z\alpha$ – $Z\beta$. **a** Overlay of the 1H – ^{15}N HSQC spectra of $Z\alpha$, $Z\beta$ and $Z\alpha$ – $Z\beta$ in green, blue, and purple, respectively. **b** Chemical shift perturbations (CSPs) (Montaville et al. 2008; Williamson 2013) between the isolated $Z\alpha$ and $Z\beta$ domains versus the domains within the con-

text of $Z\alpha$ – $Z\beta$. Residues which showed CSP values above 0.19 were considered to be significant. ${\bf c}$ Residues which showed significant CSPs from ${\bf b}$ are plotted (residues colored red) onto the structures of $Z\alpha$ (green, PDB ID: 2GXB, (Placido et al. 2007)) and $Z\beta$ (blue, PDB ID: 1XMK, (Athanasiadis et al. 2018))



Acknowledgements The authors thank David Jones (University of Colorado, Aurora) for help with NMR spectroscopy, and Jeffrey Kieft for support. This project was supported by NIH Grant R01GM130694-01A1, NSF Grant 1917254 for Infrastructure Innovation for Biological Research, and a start-up package by the University of Colorado to B.V., and University of Colorado Cancer Center Support Grant P30 CA046934 and NIH Biomedical Research Support Shared Grant S10 OD025020-01.

Data availability The chemical shift assignments for $Z\alpha$ (BMRB 50714), $Z\beta$ (BMRB 50713) and $Z\alpha$ – $Z\beta$ (BMRB 50715) have been deposited in the Biological Magnetic Resonance Data Bank.

Declarations

Conflict of interest The authors declare they have no conflict of interest.

References

- Athanasiadis A (2012) Zalpha-domains: At the intersection between RNA editing and innate immunity. Semin Cell Dev Biol 23:275–280
- Athanasiadis A, Placido D, Maas S, Brown BA, Lowenhaupt K, Rich A (2005) The crystal structure of the Zβ domain of the RNA-editing enzyme ADAR1 reveals distinct conserved surfaces among Z-domains. J Mol Biol 351(3):496–507
- Bass BL, Weintraub H (1988) An unwinding activity that covalently modifies its double-stranded RNA substrate. Cell. https://doi.org/ 10.1016/0092-8674(88)90253-X
- Brown BA, Lowenhaupt K, Wilbert CM et al (2000) The Zα domain of the editing enzyme dsRNA adenosine deaminase binds left-handed Z-RNA as well as Z-DNA. Proc Natl Acad Sci USA. https://doi.org/10.1073/pnas.240464097
- Cai M, Huang Y, Yang R et al (2016) A simple and robust protocol for high-yield expression of perdeuterated proteins in *Escherichia coli* grown in shaker flasks. J Biomol NMR. https://doi.org/10.1007/s10858-016-0052-y
- Cavanagh J (2007) Protein NMR spectroscopy: principles and practice.

 Academic Press, London
- Chung H, Calis JJA, Wu X et al (2018) Human ADAR1 prevents endogenous RNA from triggering translational shutdown. Cell. https://doi.org/10.1016/j.cell.2017.12.038
- Delaglio F, Grzesiek S, Vuister GW et al (1995) NMRPipe: a multidimensional spectral processing system based on UNIX pipes. J Biomol NMR 6:277–293. https://doi.org/10.1007/BF00197809
- George CX, Samuel CE (1999) Human RNA-specific adenosine deaminase ADAR1 transcripts possess alternative exon 1 structures that initiate from different promoters, one constitutively active and the other interferon inducible. Proc Natl Acad Sci USA. https://doi.org/10.1073/pnas.96.8.4621
- Herbert A, Schade M, Lowenhaupt K et al (1998) The Zα domain from human ADAR1 binds to the Z-DNA conformer of many different sequences. Nucleic Acids Res. https://doi.org/10.1093/nar/26.15.3486
- Hyberts SG, Milbradt AG, Wagner AB et al (2012) Application of iterative soft thresholding for fast reconstruction of NMR data non-uniformly sampled with multidimensional Poisson Gap scheduling. J Biomol NMR. https://doi.org/10.1007/s10858-012-9611-z

- Kruse H, Mrazikova K, D'Ascenzo L et al (2020) Short but weak: the Z-DNA Lone-Pair···π conundrum challenges standard carbon Van der Waals radii. Angew Chemie Int Ed. https://doi.org/10.1002/anie.202004201
- Lee W, Tonelli M, Markley JL (2015) NMRFAM-SPARKY: enhanced software for biomolecular NMR spectroscopy. Bioinformatics 31:1325–1327. https://doi.org/10.1093/bioinformatics/btu830
- Marsh JA, Singh VK, Jia Z, Forman-Kay JD (2006) Sensitivity of secondary structure propensities to sequence differences between α-and γ-synuclein: implications for fibrillation. Protein Sci. https://doi.org/10.1110/ps.062465306
- Montaville P, Coudevylle N, Radhakrishnan A et al (2008) The PIP2 binding mode of the C2 domains of rabphilin-3A. Protein Sci. https://doi.org/10.1110/ps.073326608
- Nishikura K (2016) A-to-I editing of coding and non-coding RNAs by ADARs. Nat Rev Mol Cell Biol 17:83–96
- O'Connell MA, Keller W (1994) Purification and properties of doublestranded RNA-specific adenosine deaminase from calf thymus. Proc Natl Acad Sci USA. https://doi.org/10.1073/pnas.91.22. 10596
- O'Connell MA, Krause S, Higuchi M et al (1995) Cloning of cDNAs encoding mammalian double-stranded RNA-specific adenosine deaminase. Mol Cell Biol. https://doi.org/10.1128/mcb.15.3.1389
- Patterson JB, Samual SE (1995) Expression and regulation by interferon of a double-stranded-RNA-specific adenosine deaminase from human cells: evidence for two forms of the deaminase. Mol Cell Biol 15:5376–5388
- Placido D, Brown BA, Lowenhaupt K et al (2007) A left-handed RNA double helix bound by the Zα domain of the RNA-editing enzyme ADAR1. Structure. https://doi.org/10.1016/j.str.2007.03.001
- Schade M, Turner CJ, Kühne R et al (1999a) The solution structure of the Za domain of the human RNA editing enzyme ADAR1 reveals a prepositioned binding surface for Z-DNA. Proc Natl Acad Sci USA. https://doi.org/10.1073/pnas.96.22.12465
- Schade M, Turner CJ, Lowenhaupt K et al (1999b) Structure-function analysis of the Z-DNA-binding domain $Z\alpha$ of dsRNA adenosine deaminase type I reveals similarity to the $(\alpha + \beta)$ family of helix-turn-helix proteins. EMBO J. https://doi.org/10.1093/emboj/18.2. 470
- Schwartz T, Lowenhaupt K, Kim YG et al (1999a) Proteolytic dissection of Zab, the Z-DNA-binding domain of human ADAR1. J Biol Chem. https://doi.org/10.1074/jbc.274.5.2899
- Schwartz T, Rould MA, Lowenhaupt K et al (1999b) Crystal structure of the Zalpha domain of the human editing enzyme ADAR1 bound to left-handed Z-DNA. Science 11:1841–1845
- Vranken WF, Boucher W, Stevens TJ et al (2005) The CCPN data model for NMR spectroscopy: development of a software pipeline. Proteins Struct Funct Genet 59:687–696. https://doi.org/10. 1002/prot.20449
- Wagner RW, Smith JE, Cooperman BS, Nishikura K (1989) A doublestranded RNA unwinding activity introduces structural alterations by means of adenosine to inosine conversions in mammalian cells and Xenopus eggs. Proc Natl Acad Sci USA. https://doi.org/10. 1073/pnas.86.8.2647
- Williamson MP (2013) Using chemical shift perturbation to characterise ligand binding. Progr Nuclear Magn Reson Spectrosc 73:1–6

Publisher's Note Springer Nature remains neutral with regard to jurisdictional claims in published maps and institutional affiliations.

